Periplasmic expression of Pseudomonas fluorescens peroxidase Dyp1B and site-directed mutant Dyp1B enzymes enhances polymeric lignin degradation activity in Pseudomonas putida KT2440

Ehibhatiomhan, A. O., Pour, R. R., Farnaud, S., Bugg, T. D. H. & Mendel-Williams, S.

Original citation:
Ehibhatiomhan, AO, Pour, RR, Farnaud, S, Bugg, TDH & Mendel-Williams, S 2023, 'Periplasmic expression of Pseudomonas fluorescens peroxidase Dyp1B and site-directed mutant Dyp1B enzymes enhances polymeric lignin degradation activity in Pseudomonas putida KT2440', *Enzyme and Microbial Technology*, vol. 162, 110147. https://dx.doi.org/10.1016/j.enzmictec.2022.110147

DOI 10.1016/j.enzmictec.2022.110147
ISSN 0141-0229
ESSN 1879-0909

Publisher: Elsevier

Enzyme and Microbial Technology 162 (2023) 110147

Contents lists available at ScienceDirect

Enzyme and Microbial Technology

journal homepage: www.elsevier.com/locate/enzmictec

Periplasmic expression of *Pseudomonas fluorescens* peroxidase Dyp1B and site-directed mutant Dyp1B enzymes enhances polymeric lignin degradation activity in *Pseudomonas putida* KT2440

Austine O. Ehibhatiomhan [a], Rahman Rahman Pour [b], Sebastien Farnaud [a], Timothy D.H. Bugg [b,*], Sharon Mendel-Williams [a,*]

[a] School of Life Sciences, Coventry University, Coventry CV1 5FB, UK
[b] Department of Chemistry, University of Warwick, Coventry CV4 7AL, UK

ARTICLE INFO

Keywords:
Dye-decolorizing peroxidases
Manganese oxidation
Lignin degradation
Pseudomonas fluorescens
Pseudomonas putida

ABSTRACT

Expression of lignin-oxidising *Pseudomonas fluorescens* Dyp1B in the periplasm of *Pseudomonas putida* KT2440, using a *tat* fusion construct, was found to lead to enhanced whole cell activity for oxidation of DCP and polymeric lignin substrates. Four amino acid residues predicted to lie at the manganese ion binding site of *Pseudomonas fluorescens* peroxidase Dyp1B were investigated using site-directed mutagenesis. Mutants H127R and S223A showed 2-fold and 4-fold higher k_{cat} for Mn(II) oxidation respectively, and mutant S223A showed 2-fold enhanced production of low molecular weight phenolic products from a polymeric soda lignin. The mutant Pfl Dyp1B genes were expressed as *tat* fusions to investigate their effect on lignin oxidation by *P. putida* KT2440.

1. Introduction

The aromatic heteropolymer lignin is, together with cellulose and hemi-cellulose, a major component of the lignocellulose plant cell wall, and comprises 15–30% of plant biomass [1]. Hence there is considerable interest in the conversion of lignin into renewable aromatic chemicals, either using chemical catalysis or biocatalysis [2]. Microbial enzymes that are able to attack lignin include fungal lignin peroxidase and manganese peroxidase enzymes secreted by white-rot Basidiomycete fungi, and fungal multi-copper oxidase enzymes [3]. Bacterial enzymes have also been identified that can attack polymeric lignin: dye-decolorizing peroxidases from *Rhodococcus jostii* RHA1 [4] and *Pseudomonas fluorescens* Pf-5 [5] show activity for polymeric lignin oxidation in the presence of Mn^{2+} ions, and further Dyp-type peroxidases with activity for lignin oxidation have been reported from *Streptomyces albidoflavus* [6] and *Pseudomonas* sp. Q18 [7]. Multicopper oxidases from *Streptomyces coelicolor* [8] and *Ochrobactrum* sp. [9] have been shown to have activity for polymeric lignin; and glutathione-dependent beta-etherase enzymes from *Sphingobium* SYK-6 and *Novosphingobium* show activity towards lignin dimers [10–12] and higher molecular weight lignin fragments [13].

Bioinformatic analysis of genomes for bacterial lignin-degrading strains has identified that nearly all such microbes contain either Dyp-type peroxidase genes or multi-copper oxidase genes on their genomes [14]. However, it is uncertain whether Dyp-type peroxidases are expressed extracellularly or intracellularly: A-type Dyp sequences contain a Tat signal sequence for protein export [14], but B-type Dyp peroxidases that contain lignin-oxidising enzymes are either targeted to an encapsulin nanocompartment [15], or contain no signal sequence. Since the initial steps of lignin oxidation must be extracellular, then we hypothesised that expression of lignin-oxidising enzymes either extracellularly or in periplasm of Gram-negative bacteria may improve microbial lignin oxidation. As precedent, it has been reported that overexpression of *Streptomyces* small laccase SLAC leads to enhancement in the rate of acid-precipitable polymeric lignin (APPL) production in *Streptomyces coelicolor* [16]. Also in a plant host, overexpression of *R. jostii* DypB in tobacco is reported to cause reduced lignin content [17]. Hence we wished to investigate whether extracellular or periplasmic expression of a Dyp-type peroxidase with activity for lignin oxidation would cause enhancement in microbial lignin breakdown.

We have also investigated amino acid replacements at the active site of a Dyp-type peroxidase that could further enhance lignin oxidation activity. The active site of DyP-type peroxidases contains catalytic aspartic acid and arginine residues responsible for the formation of the

* Corresponding authors.
E-mail addresses: T.D.Bugg@warwick.ac.uk (T.D.H. Bugg), Sharon.Williams@coventry.ac.uk (S. Mendel-Williams).

https://doi.org/10.1016/j.enzmictec.2022.110147
Received 14 July 2022; Received in revised form 14 October 2022; Accepted 18 October 2022
Available online 20 October 2022

compound I iron-oxo intermediate responsible for substrate oxidation, whose function have been explored via site-directed mutagenesis and spectroscopic studies [18–21]. In B-type DyP peroxidases which have activity for Mn^{2+} oxidation, there is a Mn^{2+} binding site adjacent to the haem edge, whose structure has been determined in *R. jostii* RHA1 DypB [4]. Replacement of an Asn-246 residue by Ala in *R. jostii* DypB led to an 80-fold increase in k_{cat} for Mn^{2+} oxidation [22]. Mn^{3+} is thought to act as a diffusible oxidant that can penetrate the lignin structure to initiate lignin depolymerisation. Given the modest activity of bacterial DyP-type peroxidases towards phenolic substrates (k_{cat}/K_M 10^2-10^3 $M^{-1}s^{-1}$) and Mn^{2+} (k_{cat}/K_M 10^2-10^3 $M^{-1}s^{-1}$), studies to improve activity by protein engineering have been reported. Error-prone polymerase chain reaction has been used to enhance the activity of *Pseudomonas putida* DyP, identifying three mutations on the surface of the protein (E188K, A142V, H12V) that enhance k_{cat}/K_M for 2,6-dimethoxyphenol by 100-fold, and move the optimum pH to 8.5 [23]. Directed evolution using focused libraries at the active site of *Pseudomonas fluorescens* Pf-5 DyP1B identified mutant H169L which showed enhanced low molecular weight product release from polymeric lignin [24]. Directed evolution of *Pleurotus ostreatus* Dyp4 has also been reported, via fusion of the Dyp4 gene with *E. coli* OsmY, an extracellular protein [25].

Since *Pseudomonas putida* KT2440 has activity for lignin breakdown, and expression systems for this bacterium are well developed, we investigated the expression of Dyp1B either in the periplasm or on the outer membrane of this bacterium. Here we report the expression of *P. fluorescens* DyP1B and mutant DyP1B enzymes in the periplasm of lignin-degrading bacterium *Pseudomonas putida* KT2440. We have investigated four amino acid replacements at the manganese ion binding site of *P. fluorescens* DyP1B, in order to enhance activity for Mn^{2+} oxidation.

2. Materials and methods

2.1. Construction of TAT-Dyp1B fusion

The TAT signal sequence of *Thermobifida fusca* DyP peroxidase (Uniprot accession Q47KB1, amino acids 1–46) was amplified by polymerase chain reaction (nucleotide primers given in Supporting Information Table S1), together with a His_6 fusion tag, and cloned using restriction enzymes *Hin*dIII and *Pst*I into the polylinker site of plasmid pIZ1016 [26] to make a pIZ1016-TAT construct. The *Pseudomonas fluorescens* Dyp1B gene (Uniprot accession Q4KAC6_PSEF5) was then amplified by polymerase chain reaction (nucleotide primers given in Supporting Information Table S1), and cloned into pIZ1016-TAT using restriction enzymes *Pst*I and *Xba*I to make the pIZ1016-TAT-Dyp1B construct, whose nucleotide sequence was verified by DNA sequencing. Assembled pIZ1016_*Tfutatsp_dyp1B* constructs were transformed into Agilent *E. coli* XL1-blue competent cells. The plasmid was transformed into *Pseudomonas putida* KT2440 via electroporation (Bio-Rad Gene Pulser, 2.5 kV).

2.2. Construction of OprF-Dyp1B fusion

A synthetic gene containing a truncated *Pseudomonas aeruginosa* OprF gene (Uniprot accession P13794, sequence up to Lys-165) fused to the *Pseudomonas fluorescens* Dyp1B gene (Uniprot accession Q4KAC6_PSEF5) was purchased from Genscript, in a pUC19 vector. This 1.4 kb synthetic gene was excised using restriction enzymes *Sal*I and *Pst*I, and cloned into the polylinker site of pIZ1016 to make the pIZ1016-OprF-Dyp1B construct. The plasmid was transformed into *Pseudomonas putida* KT2440 via electroporation (Bio-Rad Gene Pulser, 2.5 kV).

2.3. Growth of P. putida KT2440 expressing TAT-Dyp1B fusions

All components of the growth media were prepared individually and were either autoclaved or where appropriate, filter sterilized. Cultures of *P. putida* KT2440 cells maintaining pIZ1016_*Tfutatsp_dyp1B* constructs were grown in M9 media from Sigma-Aldrich supplemented with trace elements ($FeSO_4$0.7 H_2O, $ZnSO_4$0.7 H_2O, $MnSO_4{\cdot}H_2O$, H_3BO_3, $NiCl_2$0.6 H_2O, EDTA, $CoCl_2$0.6 H_2O, $CuCl_2$0.2 H_2O, $NaMoO_4$0.2 H_2O, and Na-EDTA) in a shake flask incubator. A final concentration of 0.3 % (w/v) Protobind lignin (Green Value Ltd) was utilised as the main carbon source. The M9 growth medium was further supplemented with 0.4 % (w/v) glucose, 1 mM $MgSO_4$, 0.3 mM $CaCl_2$, 0.25 % (w/v) yeast extract, 1 mM $MnSO_4$, 0.5 mM IPTG, and 15 mg/mL gentamycin where applicable. A final concentration of 1 mM H_2O_2 was added to cultures at inoculation and then every 24 h. The growth cultures were incubated on a constant shaker at 30 °C for 168 h. Samples were aseptically extracted every 24 h for metabolic product analysis, and cell growth was estimated via colony forming units.

2.4. Construction of site-directed mutant Dyp1B enzymes

A previously designed pET151*Pfdyp1B* construct [5] was utilised as the DNA template for the site-directed mutagenesis of selected amino acid residues, using the New England BioLabs (NEB) Q5® Site-Directed Mutagenesis Kit for mutants E137A, E195A, S223A and H127R/S223N, and QuikChange II Site-Directed Mutagenesis Kit (Stratagene Agilent technologies) for mutants H127R and S223N. Each amino acid substitution was performed using a pair of designed primers containing the desired amino acid flanked by sequences complementary to the *Pfdyp1B* gene. Primers are shown in Supporting Information Table S1. PCR reactions were carried out using materials provided in each manufacturers kit and according to instructions laid out by both manufacturers. Amplified constructs housing the mutant *Pfdyp1B* genes were subjected to *Dpn*I digestion using the NEB KLD enzyme mix. Following digestion PCR products were transformed into Agilent *E. coli* XL1-blue competent cells. The extracted plasmids from obtained colonies were sent for sequencing in order to confirm the accuracy of the sequence and that amplified constructs did not contain any undesired mutations. Sequencing results confirmed the presence of the desired mutations and the absence of any undesired mutations. Following sequencing, the recombinant plasmids were transformed into NEB BL21 competent *E. coli* for protein expression. For the expression of the recombinant *Pfdyp1B* variants genes, 20 mL starter cultures of Luria–Bertani broth were inoculated with single colonies of each variant in the presence of 100 mg/mL ampicillin and incubated overnight at 37 °C. Overnight cultures were then added to 1 L Luria–Bertani broth and incubated at 37 °C until OD at 600 nm was 0.6–0.8 A.U. Finally, cells were induced by adding Isopropyl β-D-1-thiogalactopyranoside (IPTG) at a final concentration 1 mM and shaken overnight at room temperature (≈20 °C), 60 rpm. Cell pellets were harvested by centrifugation at 4000xg for protein purification.

2.5. Purification of recombinant Dyp1B enzymes

Protein purification was carried out by metal affinity chromatography. Extracted cell pellets were re-suspended in 20 mL lysis buffer (50 mM NaH_2PO_4, 300 mM NaCl, and 10 mM imidazole at pH 8) in the presence of phenylmethanesulfonylfluoride (PMSF) at a final concentration of 1 mM. Cells were lysed using a constant system cell disruptor, followed by centrifugation at 10,000xg for 30 min, clear supernatant containing extracted proteins was collected. Each extracted protein solution was filtered and loaded onto a Ni-NTA resin FPLC column (HisTrap Excel, 1 mL) equilibrated with lysis buffer, washed using wash buffer (50 mM NaH_2PO_4, 300 mM NaCl, and 20 mM imidazole at pH 8), and the recombinant protein was eluted by 10 mL of elution buffer (50 mM NaH_2PO_4, 300 mM NaCl, and 500 mM imidazole at pH 8). Protein aliquots were subjected to SDS-PAGE electrophoresis and spectrophotometry analysis using the Thermo Scientific NanoDrop spectrophotometer. Remaining protein samples were put through buffer exchange using a PD-10 de-salting column and eluted into MOPS buffer (80 mM

NaCl and 20 mM MOPS at pH 7.5).

2.0 M equivalents of heme dissolved in DMSO was mixed vigorously with protein solutions and incubated at room temperature for 2 h, excess heme was removed by centrifugation at 10,000xg for 30 min. Following heme reconstruction, aliquots of samples were passed through a PD-10 column equilibrated by and eluted into 10 mM K_3PO_4 buffer pH 8.0. Eluted proteins were loaded into a Jasco T-1500 Circular dichroism spectrometer with a path length of 1 mm, and circular dichroism spectra were obtained following monitoring at 190–300 nm. Protein samples were subsequently passed through a PD-10 column equilibrated by and eluted into 20 mM MOPS pH 7.5 containing 80 mM NaCl.

2.6. Assay of Dyp1B enzymes

Assays were performed at 25 °C in 100 mM acetate buffer pH 5.5 using a Hidex microplate reader. Kinetic parameters (k_{cat} and K_M) were determined by nonlinear curve fitting to the obtained enzyme activity, using Graphpad prism 5 software, fitting to the Michaelis–Menten equation. All assays were performed in triplicate, and standard error determined from curve fitting.

Oxidation of DCP (2,4-dichlorophenol) was assayed over concentration range 10 μM–6 mM in the presence of 1 mM hydrogen peroxide, monitoring at 510 nm (ε 18,000 M^{-1} cm^{-1}). Oxidation of ABTS (2,20-azino-bis(3-ethylbenzothiazoline-6-sulphonic acid) was assayed in the presence of 1 mM hydrogen peroxide over concentration range 25 μM–6 mM, monitoring at 420 nm (ε 36,000 M^{-1} cm^{-1}). Oxidation of Mn^{2+} was assayed in 100 mM sodium tartrate buffer (pH 5.5) with 1 mM hydrogen peroxide using 100 μM–6 mM $MnCl_2$, monitoring at 238 nm (ε 6500 M^{-1} cm^{-1}). Oxidation of alkali Kraft lignin (Sigma-Aldrich) was performed with 50 μM Kraft lignin and 1 mM hydrogen peroxide in the presence of 2 mM Dyp1B enzyme (engineered or wild type), monitoring at 465 nm.

2.7. Assay of polymeric lignin oxidation

Powdered Green Value Protobind lignin (25 mg) was dissolved in DMSO (1 mL), and 30 μL was added to succinate buffer (3 mL, 50 mM, pH 5.5), followed by addition of DyP1B (wild type or selected mutant) (100 μL, 1 mg/mL) and hydrogen peroxide (1 mM). The resulting solution was incubated at room temperature for 1–24 hr at 30 °C. For detection of aldehyde and ketone products, assay was adapted from reference 27]. Samples (20 μL) were mixed with 0.1 M HCl (30 μL) and 2, 4-dinitrophenylhydrazine (DNP) (50 μL, 1 mM solution in 0.1 M HCl), then incubated for a further 5 min at room temperature. 0.1 M NaOH (100 μL) was added, and the absorbance at 450 nm measured using a HIDEX Sense microtitre platereader. For detection of phenolic products, assay was adapted from reference 28]. Samples (20 μL) were mixed with distilled water (100 μL) and Folin-Ciocalteu reagent (Sigma-Aldrich) (10 μL), then 4 % Na_2CO_3 (100 μL) was added after 4 min, then incubated in the dark for 30 min at room temperature. Absorbance at 750 nm measured using a HIDEX Sense microtitre platereader.

For HPLC analysis, the reaction was stopped by adding 1 M HCl (10 μL), and reaction products were extracted into ethyl acetate (6 mL), and the mixture was centrifuged for 5 min at 10,000 rpm. The organic layer was removed, evaporated and the residue was dissolved in methanol. HPLC analysis was conducted using a Phenomenex Luna 5 μm C18 reverse phase column (100Å, 50 mm, 4.6 mm) on a Hewlett-Packard Series 1100 analyzer, at a flow rate of 0.5 mL/min, monitoring at 310 nm. The gradient was as follows: 10–30 % MeOH/H_2O over 10 min, 30–40 % MeOH/H_2O from 10 to 20 min, 40–70 % MeOH/H_2O from 20 to 30 min and 70–100 % MeOH/H_2O from 30 to 40 min

3. Results

3.1. Expression of Dyp1B in periplasm of Pseudomonas putida KT2440

Unlike *R. jostii* RHA1 DypB, which contains a C-terminal signal sequence for targeting to a bacterial nanocompartment known as encapsulin [15], *P. fluorescens* Dyp1B contains no C-terminal targeting sequence, and appears to have no signal sequence for protein export [4]. In order to export to the periplasm of *P. putida* KT2440, the TAT protein secretion system was used, a strategy that has been used previously to target organophosphate hydrolase to the periplasm [29]. A TAT signal sequence was fused to the 3' end of the *dyp1B* gene, and the construct was expressed on the pIZ1016 expression vector [26], under the control of a Ptac promoter (see Supporting information Fig. S1 for plasmid map). pIZ1016_TAT-Dyp1B was then transformed into *P. putida* KT2440. Expression with 1 mM IPTG led to the appearance of two new protein bands in the periplasmic fraction, corresponding to unprocessed Dyp1B and processed Dyp1B (see Fig. 1A). Dyp1B was also expressed intracellularly, via a pIZ1016_Dyp1B construct.

In order to display on the cell surface of *P. putida* KT2440, the *dyp1B* gene was fused to the *oprF* gene encoding outer membrane protein OprF from *Pseudomonas aeruginosa*, which has been used to display epitope tags [30] and SIK W1 lipase [31] extracellularly. The *dyp1B* gene was fused onto the C-terminus of a truncated OprF, as reported previously [31]. pIZ1016_OprF-Dyp1B was then transformed into *P. putida* KT2440. Expression with 1 mM IPTG led to the appearance of a new protein band at 51 kDa in the membrane fraction, corresponding to the OprF-Dyp1B fusion (see Supporting information Fig. S2).

These constructs were then assayed for activity against a phenolic substrate and a lignin substrate. Whole cells induced with 0.5 mM IPTG were incubated with peroxidase substrate 2,4-dichlorophenol (DCP), and absorbance change at 510 nm measured. As shown in Fig. 1B, wild-type *P. putida* KT2440 or KT2440 containing intracellular Dyp1B showed no detectable activity, however, the TAT-Dyp1B construct showed DCP oxidation activity, whereas the OprF-Dyp1B construct showed no activity. These data implied that the TAT-Dyp1B construct had successfully exported Dyp1B in active form, but the OprF-Dyp1B fusion was either misfolded or inactive.

In order to assess lignin oxidation activity, we have used a colorimetric assay for low molecular weight phenolic products (see Fig. 1C), which we have previously applied to lignin-oxidising enzymes [28]. The *P. putida* constructs containing TAT-Dyp1B and OprF-Dyp1B were grown on minimal M9 media containing 1 % milled miscanthus lignocellulose for 24 hr at 30 °C after induction with 0.5 mM IPTG, in the presence and absence of 0.5 mM $MnCl_2$. Aliquots were removed, and small molecule phenolic products were detected using the Folin-Ciocalteu assay [28], as shown in Fig. 1. Wild-type *P. putida* KT2440 showed a low level of activity, which was not dependent on Mn^{2+}, whereas the TAT-Dyp1B construct showed approximately 10-fold higher activity (see Fig. 1D) in the presence of Mn^{2+}. There was no detectable activity with the OprF-Dyp1B construct. In order to confirm delignification, we further analysed the lignin content of the treated lignocellulose using the Klason assay. Untreated lignocellulose contained 37.0 ± 0.5 % lignin; treatment with wild-type *P. putida* KT2440 gave 36.6 ± 0.5 % lignin; and treatment with KT2440/pIZ1016_TAT-Dyp1B gave 35.0 ± 0.5 % lignin, corresponding to 5.4 % delignification.

3.2. Site-directed mutagenesis at the manganese ion binding site of Pfl Dyp1B

Since the activity of Dyp1B towards polymeric lignin and lignocellulose is enhanced by Mn^{2+}, we investigated amino acid replacements at the predicted manganese ion binding site, in order to enhance lignin oxidation activity. The manganese ion binding site of *R. jostii* RHA1 DypB determined by X-ray crystallography involves Glu-156, Glu-215, Glu-239 and a heme propionate as ligands [22]. Amino acid sequence alignment of these residues with other B-type DyP peroxidases indicates that Glu-156 (found as Glu-137 in Pfl DyP1B) and Glu-215 (found as Glu-195 in Pfl Dyp1B) are conserved residues, whereas Glu-239 is found as Gly or Ser in 3 out of 8 sequences (see Fig. 2). A homology model constructed previously for *P. fluorescens* DyP1B (see Supporting

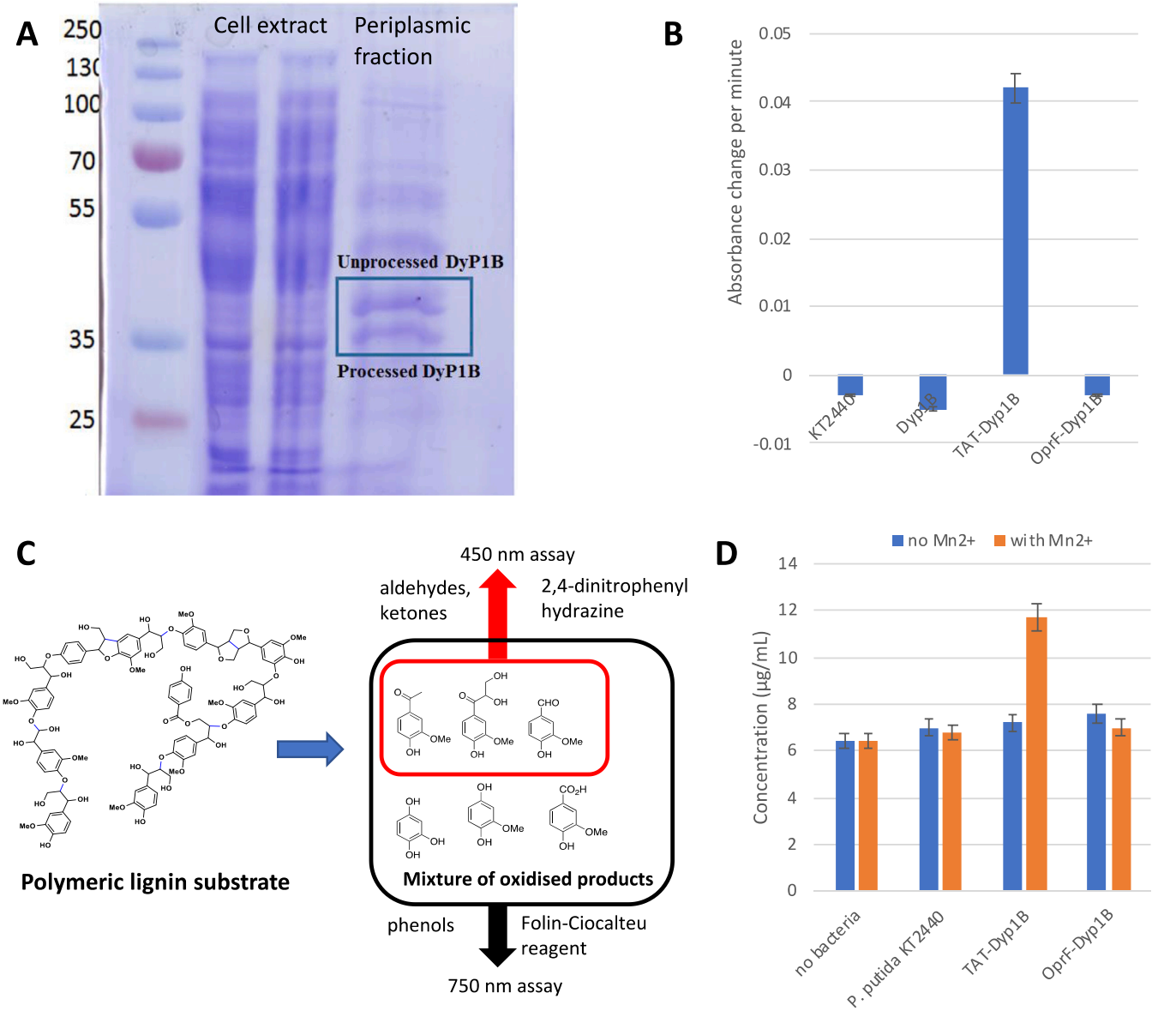

Fig. 1. Expression and activity of TAT-Dyp1B in periplasm of *Pseudomonas putida* KT2440. (A) Heterologous expression of recombinant TAT-Dyp1B in periplasm of *P. putida* KT2440. (B) Activity of whole cell *P. putida* TAT-Dyp1B and OprF-Dyp1B constructs for oxidation of phenolic substrate DCP. (C) Assays for small molecule phenolic products from polymeric lignin or lignocellulose. (D) Activity of whole cell *P. putida* KT2440 expressing TAT-Dyp1B for low molecular weight phenol production from miscanthus lignocellulose, using Folin-Ciocalteu assay. Concentration of phenolic products was estimated using a calibration curve of 5–100 µg/mL catechol.

information Fig. S4) indicated that His-127 and Ser-223 might be positioned closer to Mn^{2+} in this enzyme [24]. His-127 is conserved in 2 DyP sequences, and is replaced by Arg in 6 other sequences. Ser-223 is conserved in 5 DyP sequences, and replaced by Asn in 2 sequences, and Ala in one sequence. In *R. jostii* RHA1 DyPB, this amino acid is Asn-246, whose replacement by Ala leads to increased activity [22]. We have previously prepared H127R and S223N mutant DyP1B enzymes, which show 3-fold increased k_{cat} for Mn^{2+} oxidation [24], and in addition we have made further E137A, E195A, S223A mutants and a H127R/S223N double mutant.

H127R, E137A, E195A, S223A, S223N, and S223N/H127R mutant DyP1B enzymes were expressed as His_6 fusion proteins, and purified by Ni-NTA affinity chromatography (SDS-PAGE gels shown in Supporting information Figure S5-S11). Yields of purified protein were in the range 3–6.5 mg per litre cell culture. The purified enzymes were analysed by circular dichroism spectroscopy, verifying that no significant changes in secondary structure had occurred as a result of amino acid replacements (see Figure S12 and Table S2 in Supporting information).

The mutant enzymes, together with the S223N and H127R mutant enzymes reported previously, were assayed against ABTS, DCP and Mn (II) substrates, and kinetic constants K_M and k_{cat} were determined (see Table 1).

Mutations H127R, S223A and S223N confer increased k_{cat} towards DCP and Mn^{2+} substrates, with S223A showing 8-fold increased k_{cat}/K_M for Mn^{2+}oxidation. Mutations E137A and E195A show 5–8 fold reduced k_{cat}/K_M for Mn^{2+} oxidation, with E137A showing a 3-fold higher K_M for Mn^{2+}, consistent with the involvement of Glu-137 and Glu-195 at the manganese ion binding site.

In order to test whether the effects on Mn^{2+} oxidation also led to enhanced lignin oxidation activity, two different assay methods were used to study oxidation of polymeric lignin. We have found previously that treatment of alkali Kraft lignin (Sigma-Aldrich) with either *R. jostii* RHA1 DypB [4] or *P. fluorescens* Dyp1B [5] leads to an increase in absorbance at 465 nm, which exhibits Michaelis-Menten kinetic

P. fluorescens DyP1B	*His*^{127}	Glu^{137}	Glu^{195}	Glu^{216}	*Ser*^{223}
P. putida KT2440 DyP	His	Glu	Glu	Glu	Ser
R. jostii RHA1 DyPB	Arg^{146}	**Glu^{156}**	**Glu^{215}**	**Glu^{239}**	Asn^{246}
S. viridochromogenes DyP	Arg	Glu	Glu	Glu	Ala
K. pneumoniae DyP	Arg	Glu	Glu	Gly	Ser
E. lignolyticus SCF1 DyP	Arg	Glu	Glu	Gly	Ser
S. oneidensis MR-1 DyP	Arg	Glu	Glu	Ser	Ser
M. phosphovorus DyP	Arg	Glu	Glu	Glu	Asn

Fig. 2. Amino acid sequence alignment of amino acid residues implicated at the manganese ion binding site of B-type DyP peroxidases, either by X-ray crystallography in *R. jostii* RHA1 DyPB [22] (marked in bold), or by homology model in *P. fluorescens* DyP1B [24] (in italics). Full amino acid sequence alignment is given in Supporting information Fig. S3, homology model illustrated in Fig. S4.

behaviour. Each of the mutant Pfl Dyp1B site-directed mutant enzymes were assayed against alkali Kraft lignin in this way, and the results are shown in Fig. 3. Activity was dependent upon addition of 3 mM $MnSO_4$ to the assay, and increased activity was observed for H127R, S223N and S223A mutants, with highest activity by mutant S223A. Mutants E137A and E195A showed no significant increase in activity in the presence of $MnSO_4$, consistent with weak Mn^{2+} oxidation.

Each mutant enzyme was also assayed against Green Value Protobind lignin, a commercially available soda lignin manufactured from a wheat/sarkanda grass, using 2,4-dinitrophenylhydrazine to detect the production of low molecular weight aldehyde & ketone products. This assay has been previously validated using a set of lignin-oxidising enzymes and polymeric lignins, showing time-dependent and protein-dependent increases in absorbance [27,28]. Mutants S223N and S223A showed higher activity than wild-type Dyp1B, with S223A showing highest activity, approximately 2-fold higher than wild-type Dyp1B. Analysis of the extracted products by HPLC revealed enhanced production of several product peaks by S223N and S223A enzymes, including vanillin at retention time 19.6 min (see Supporting information Figure S13), consistent with the data in Fig. 4.

Each of the mutants was expressed as the TAT-Dyp1B fusion in *P. putida* KT2440. Whole cells expressing each TAT-Dyp1B fusion were used to treat Green Value Protobind lignin, and the formation of low molecular weight products was quantitated using two colorimetric assays reported previously: the Folin-Ciocalteu assay for low molecular weight phenols (see Fig. 5A), and 2,4-dinitrophenylhydrazine to detect aldehyde & ketone products (see Fig. 5B). As shown in Fig. 5, the presence of a periplasmic DyP1B enzyme was found to increase the formation of phenolic and aldehyde/ketone products by approximately 2-fold, compared with an empty vector control, and was higher than the wild-type *P. putida* KT2440 strain. However, there was no significant difference observed between the different mutant enzymes (see Discussion). Growth curves were also measured for each construct on minimal media containing 0.3 % Green Value Protobind lignin and 0.4% glucose, assessed by monitoring colony forming units vs time, which are shown in Supporting information (see Figure S14), which show slightly increased growth for all constructs expressing Dyp1B, compared to an

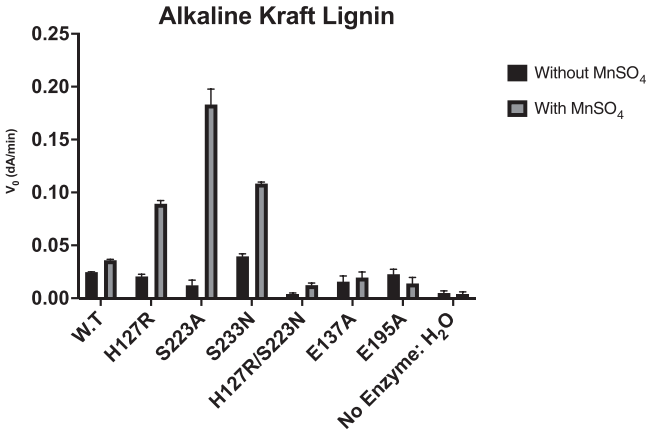

Fig. 3. Change in absorbance at 465 nm of alkali Kraft lignin treated with Pfl Dyp1B mutant enzymes. Assays contained 2 mg enzyme, and change in absorbance was measured over 5 min, as described in Materials and Methods.

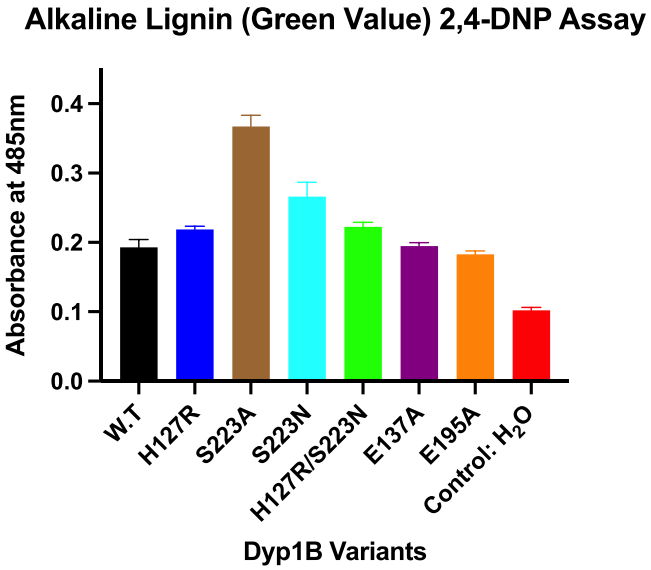

Fig. 4. Release of low molecular weight aldehyde/ketone products from Green Value Protobind lignin by treatment with Dyp1B mutant enzymes, assayed using 2,4-dinitrophenylhydrazine, in the presence of 3 mM $MnSO_4$, as described in Materials & Methods.

Table 1
Steady state kinetic data for *P. fluorescens* Dyp1B mutant enzymes. Assays carried out in triplicate, as described in Materials and Methods. Note a: for mutant S223A, saturation kinetics were not observed with ABTS as substrate, but an apparent k_{cat}/K_M value was calculated from the rate vs substrate concentration plot.

Substrate	ABTS			2,4-dichlorophenol (DCP)			$MnSO_4$		
Enzyme	k_{cat} (s^{-1})	K_M (mM)	k_{cat}/K_M ($M^{-1}s^{-1}$)	k_{cat} (s^{-1})	K_M (mM)	k_{cat}/K_M ($M^{-1}s^{-1}$)	k_{cat} (s^{-1})	K_M (mM)	k_{cat}/K_M ($M^{-1}s^{-1}$)
WT DyP1B	49 ± 1	1.65 ± 0.07	29,000	4.4 ± 0.2	1.32 ± 0.1	3300	19.8 ± 0.1	5.2 ± 0.2	3800
H127R	233 ± 1	0.43 ± 0.03	540,000	5.6 ± 0.8	0.74 ± 0.09	7600	44.3 ± 0.2	2.3 ± 0.1	19,000
E137A	97 ± 1	1.03 ± 0.03	93,000	3.8 ± 0.2	3.26 ± 0.07	1200	8.8 ± 0.8	17.6 ± 0.1	490
E195A	168 ± 3	1.09 ± 0.1	150,000	4.6 ± 0.2	1.42 ± 0.07	3300	3.8 ± 0.3	5.5 ± 0.2	690
S223A	-[a]	-[a]	17,000	8.2 ± 0.3	4.1 ± 0.2	2000	86.6 ± 0.3	2.8 ± 0.1	31,000
S223N	94 ± 1	0.28 ± 0.03	340,000	6.3 ± 0.9	0.49 ± 0.12	13,000	60.8 ± 0.2	3.8 ± 0.1	16,000
H127R/S223N	48 ± 1	1.18 ± 0.08	41,000	3.8 ± 0.9	1.17 ± 0.2	3200	6.1 ± 0.4	1.2 ± 0.1	5100

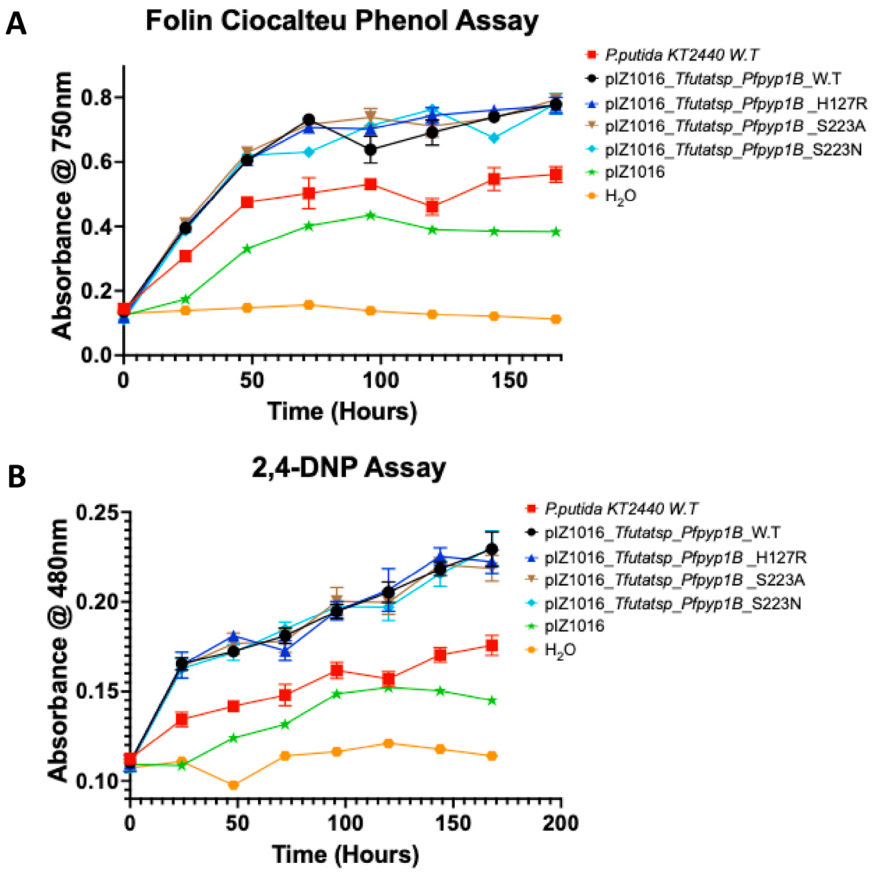

Fig. 5. Activity of *Pseudomonas putida* KT2440 expressing wild-type and mutant Tat-Dyp1B mutants against polymeric lignin, using (A) Folin-Ciocalteu assay for phenol release (B) DNP assay for aldehyde/ketone release.

empty vector control, but only minor differences between different variants.

4. Discussion

The targeting of peroxidase Dyp1B to the periplasm of *P. putida* KT2440, using the TAT protein export pathway, leads to significantly higher activity of whole cells for small molecule DCP oxidation, and generation of low molecular weight phenolic products from lignocellulose, as shown in Fig. 1. *P. putida* KT2440 is known to possess activity for lignin oxidation [32], and this microbe has been the subject of several metabolic engineering studies for generation of bioproducts from lignin degradation [33–36], hence this may be a useful approach for future engineering of *P. putida* KT2440 for breakdown of polymeric lignin. The OprF-Dyp1B fusion was found not to be active with DCP or polymeric lignin substrates, which could be due to incorrect folding of the fusion protein, proteolysis, or inaccessibility or lack of heme reconstitution of the DyP active site.

We have also investigated further amino acid replacements at the manganese ion binding site of Dyp1B, in order to improve activity for Mn^{2+} oxidation and lignin oxidation. We have found here that the S223A mutant DyP1B shows 8-fold higher k_{cat}/K_M for Mn^{2+} oxidation, compared with wild-type Dyp1B, and both S223N and S223A mutants showed higher activity for release of small molecule products from Green Value soda lignin, and higher activity towards alkali Kraft lignin. Although it is unusual that a mutation to Ala should cause enhanced activity, it is known that mutation of Asn-246 to Ala at the same position in *R. jostii* RHA1 also caused increased activity for Mn^{2+} oxidation [22]. Although Ser-223 is not likely to be a Mn^{2+} ligand, a homology model constructed previously for *P. fluorescens* DyP1B (see Supporting information Figure S4) indicated that His-127 and Ser-223 might be positioned closer to Mn^{2+} in this enzyme [24]. Possible reasons for this effect could be a re-organisation of Mn^{2+} ligands, leading to a change in the redox potential for Mn^{2+} oxidation, as observed in model complexes [37], or perhaps a change in redox potential of the heme centre [38]. Hosseinzadeh et al. have reported in 2016 that second sphere residues in a designed Mn^{2+} binding site in cytochrome c peroxidase have effects on Mn^{2+} binding and oxidation, which may relate to the effects of the S223A replacement in DyP1B [39].

The H127R mutant also showed 5-fold increased k_{cat}/K_M for Mn^{2+} oxidation. His-127 is conserved in 2 DyP sequences, and is replaced by Arg in 6 other sequences (see Fig. 2). The lower K_M for Mn^{2+} by the H127R mutant suggests some role in Mn^{2+} binding by this residue, perhaps as a second sphere residue (see Supporting information Figure S4). Replacement of Glu-137 and Glu-195 by Ala led to > 10 fold decreases in k_{cat}/K_M for Mn^{2+} oxidation, consistent with their role as Mn^{2+} ligands.

With a set of mutant enzymes, we can also examine whether there is a correlation between Mn^{2+} oxidation activity and polymeric lignin oxidation. As shown in Fig. 6, there is a correlation in this set of mutants between k_{cat}/K_M for Mn^{2+} oxidation and activity for low molecular weight phenol release from Green Value Protobind lignin, and also with the observed activity towards alkali Kraft lignin. These data provide biochemical evidence that polymeric lignin oxidation by DyP-type peroxidases is primarily via the formation of Mn^{3+}, which acts as a diffusible oxidant to attack polymeric lignin, and supports observations that DyP peroxidases showing activity for polymeric lignin oxidation are usually enzymes that can oxidise Mn^{2+} [4,5].

Expression of the wild-type and mutant Dyp1B enzymes in the periplasm of *P. putida* KT2440 gave increased conversion of polymeric lignin to low molecular weight products (see data in Fig. 5), compared with the same strain with no plasmid or with empty plasmid, confirming

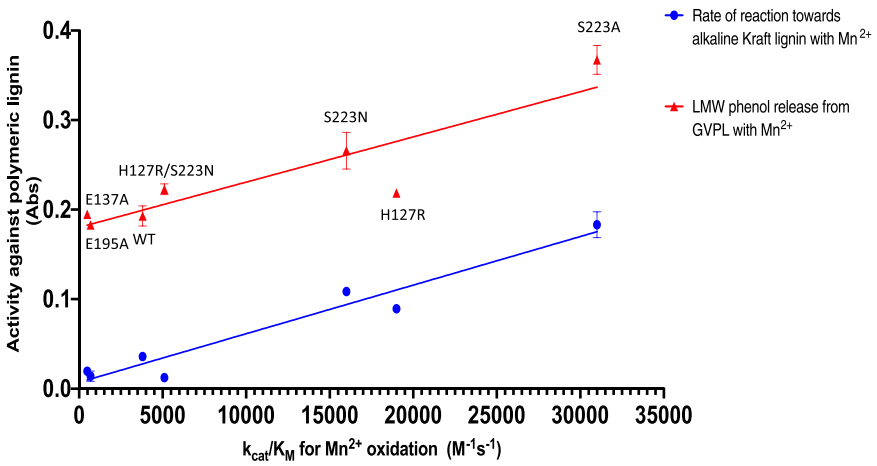

Fig. 6. Correlation between k_{cat}/K_M for Mn^{2+} oxidation and activities for polymeric lignin oxidation. Red, release of low molecular weight phenols from Green Value Protobind lignin, data from Fig. 4; blue, rate of reaction with alkali Kraft lignin, data from Fig. 3.

the lignin degradation capability of periplasmic Dyp1B. In these data there was no significant variation in product formation between the mutant and wild-type Dyp1B enzymes, even though higher activity had been observed in vitro using recombinant enzyme. It is likely that, at the cellular level, there are several enzymes and transport phenomena involved in the production of low molecular weight products from polymeric lignin. Therefore, our interpretation of this observation is that some other cellular process has become rate-limiting for lignin breakdown, which might be another enzyme, or the transport of oxidised lignin fragments, in which case the increased catalytic activity of the Dyp1B mutant does not lead to further increases in metabolite formation. We note that slightly higher growth rate on minimal media containing Green Value protobind lignin was observed for *P. putida* expressing TAT-Dyp1B-S223A (see Supporting information Figure S14), which would be consistent with a slightly higher rate of lignin oxidation.

CRediT authorship contribution statement

Austine Ehibhatiomhan and Rahman Rahman Pour carried out the research investigation; **Sharon Mendel-Williams and Timothy Bugg** obtained the research funding for the project, and conceptualised the project; **Sharon Mendel-Williams, Timothy Bugg, and Sebastien Farnaud** supervised the research project; **Austine Ehibhatiomhan, Sharon Mendel-Williams and Timothy Bugg** wrote the original draft of the manuscript.

Data availability

Data will be made available on request.

Acknowledgements

This work was supported by BBSRC ERA-IB research grant BB/M025772/1, and a Ph.D. studentship from Coventry University (to A.O.E.). We would like to thank Dr. Eduardo Díaz (CSIC Madrid) for the gift of plasmid pIZ1016, Dr. James Williamson (University of Warwick) for practical advice and assistance, and Dr Goran Rashid (University of Warwick) for assistance with HPLC.

Appendix A. Supporting information

Supplementary data associated with this article can be found in the online version at doi:10.1016/j.enzmictec.2022.110147.

References

[1] E.P. Feofilova, I.S. Mysyakina, Lignin: chemical structure, biodegradation, and practical application (a review), Appl. Biochem. Microbiol. 52 (2016) 573–581.
[2] J. Zakzeski, P.C. Bruijnincx, A.L. Jongerius, B.M. Weckhuysen, The catalytic valorization of lignin for the production of renewable chemicals, Chem. Rev. 110 (2010) 3552–3599.
[3] D.W.S. Wong, Structure and action mechanism of ligninolytic enzymes, Appl. Biochem. Biotechnol. 157 (2009) 174–209.
[4] M. Ahmad, J.N. Roberts, E.M. Hardiman, R. Singh, L.D. Eltis, T.D.H. Bugg, Identification of DypB from *Rhodococcus jostii* RHA1 as a lignin peroxidase, Biochemistry 50 (2011) 5096–5107.
[5] R. Rahmanpour, T.D.H. Bugg, Characterisation of Dyp-type peroxidases from *Pseudomonas fluorescens* Pf-5: oxidation of Mn(II) and polymeric lignin by Dyp1B, Arch. Biochem. Biophys. 574 (2015) 93–98.
[6] A. Musengi, K. Durrell, A. Prins, N. Khan, M. Agunbiade, T. Kudanga, B. Kirby-McCullough, B.I. Pletschke, S.G. Burton, M. Le, Roes-Hill. Production and characterisation of a novel actinobacterial DyP-type peroxidase and its application in coupling of phenolic monomers, Enzyme Microb. Technol. 141 (2020), 109654.
[7] C. Yang, F. Yue, Y. Cui, Y. Xu, Y. Shan, B. Liu, Y. Zhou, X. Lü, Biodegradation of lignin by *Pseudomonas* sp. Q18 and the characterization of a novel bacterial DyP-type peroxidase, in: J. Ind. Microbiol. Biotechnol., 45, 2018, pp. 913–917.
[8] S. Majumdar, T. Lukk, J.O. Solbiati, S. Bauer, S.K. Nair, J.E. Cronan, J.A. Gerlt, Roles of small laccases from Streptomyces in lignin degradation, Biochemistry 53 (2014) 4047–4058.
[9] R.S. Granja-Travez, R.C. Wilkinson, G.F. Persinoti, F.M. Squina, V. Fülöp, T.D. H. Bugg, Structural and functional characterisation of multi-copper oxidase CueO from lignin-degrading bacterium *Ochrobactrum* sp. reveal its activity towards lignin model compounds and lignosulfonate, FEBS J. 285 (2018) 1684–1700.
[10] E. Masai, A. Ichimura, Y. Sato, K. Miyauchi, Y. Katayama, M. Fukuda, Roles of enantioselective glutathione S-transferases in cleavage of β-aryl ether, J. Bacteriol. 185 (2003) 1768–1775.
[11] D.L. Gall, H. Kim, F. Lu, T.J. Donohoe, D.R. Noguera, J. Ralph, Stereochemical features of glutathione-dependent enzymes in the Sphingobium sp. strain SYK-6 β-aryl etherase pathway, J. Biol. Chem. 289 (2014) 8656–8667.
[12] D.L. Gall, J. Ralph, T.J. Donohoe, D.R. Noguera, A group of sequence-related sphingomonad enzymes catalyzes cleavage of β-aryl ether linkages in lignin β-guaiacyl and β-syringyl ether dimers, Environ. Sci. Technol. 48 (2014) 12454–12463.
[13] P. Picart, C. Müller, J. Mottweiler, L. Wiermans, C. Bolm, P. Dominguez de Maria, A. Schallmey, From gene towards selective biomass valorization: bacterial β-etherases with catalytic activity on lignin-like polymers, ChemSusChem 7 (2014) 3164–3171.
[14] R.S. Granja-Travez, G.F. Persinoti, F.M. Squina, T.D.H. Bugg, Functional genomic analysis of bacterial lignin degraders: diversity in mechanisms of lignin oxidation and metabolism, Appl. Microbiol. Biotechnol. 104 (2020) 3305–3320.
[15] R. Rahmanpour, T.D.H.Bugg Assembly, in vitro of *Rhodococcus jostii* RHA1 encapsulin and peroxidase DypB to form a nanocompartment, FEBS J. 280 (2013) 2097–2104.
[16] R. Singh, J. Hu, M.R. Regner, J.W. Round, J. Ralph, J.N. Saddler, L.D. Eltis, Enhanced delignification of steam-pretreated poplar by a bacterial laccase, Sci. Rep. 7 (2017), 42121.
[17] A. Ligaba-Osena, B. Hankoua, K. DiMarco, R. Pace, M. Crocker, J. McAtee, N. Nagachar, M. Tien, T.L. Richard, Reducing biomass recalcitrance by heterologous expression of a bacterial peroxidase in tobacco (*Nicotiana benthamiana*), Sci. Rep. 7 (2017), 17104.
[18] Y. Sugano, R. Muramatsu, A. Ichiyanagi, T. Sato, M. Shoda, DyP, a unique dye-decolorizing peroxidase, represents a novel heme peroxidase family: Asp-171

replaces the distal histidine of classical peroxidases, J. Biol. Chem. 282 (2007) 36652–36658.
[19] R. Singh, J.C. Grigg, Z. Armstrong, M.E.P. Murphy, L.D. Eltis, Distal heme pocket residues of B-type dye-decolorizing peroxidase: arginine but not aspartate is essential for peroxidase activity, J. Biol. Chem. 287 (2012) 10623–10630.
[20] V. Pfanzangl, K. Nys, M. Bellei, H. Michlits, G. Mlynek, G. Battistuzzi, K. Djinovic-Carugo, S. Van Doorslaer, P.G. Furtmüller, S. Hofbauer, C. Obinger, Roles of distal aspartate and arginine of B-class dye- decolorizing peroxidase in heterolytic hydrogen peroxide cleavage, J. Biol. Chem. 293 (2018) 14823–14838.
[21] R. Shrestha, G. Huang, D.A. Meekins, B.V. Geisbrecht, P. Li, Mechanistic insights into dye-decolorizing peroxidase revealed by solvent isotope and viscosity effects, ACS Catal. 7 (2017) 6352–6364.
[22] R. Singh, J.C. Grigg, W. Qin, J.F. Kadla, M.E.P. Murphy, L.D. Eltis, Improved manganese-oxidizing activity of DypB, a peroxidase from a lignolytic bacterium, ACS Chem. Biol. 8 (2013) 700–706.
[23] V. Brissos, D. Tavares, A.C. Sousa, M.P. Robalo, L.O. Martins, Engineering a bacterial DyP-type peroxidase for enhanced oxidation of lignin-related phenolics at alkaline pH, ACS Catal. 7 (2017) 3454–3465.
[24] R. Rahmanpour, A. Ehibhatiomhan, Y. Huang, B. Ashley, G.M.M. Rashid, S. Mendel-Williams, T.D.H. Bugg, Protein engineering of *Pseudomonas fluorescens* peroxidase Dyp1B for oxidation of phenolic and polymeric lignin substrates, Enzyme Microb. Technol. 123 (2019) 21–29.
[25] A.H.A. Alessa, K.L. Tee, D. Gonzalez-Perez, H.E.M. Omar Ali, C.A. Evans, A. Trevaskis, J.-H. Xu, T.S. Wong, Accelerated directed evolution of dye-decolorizing peroxidase using a bacterial extracellular protein secretion system (BENNY), Bioresour. Bioprocess. (6) (2019), 20.
[26] I. Martínez, M. El-Said Mohamed, D. Rozas, J.L. García, E. Díaz, Engineering synthetic bacterial consortia for enhanced desulfurization and revalorization of oil sulfur compounds, Metab. Eng. 35 (2016) 46–54.
[27] F. Tonin, E. Vignali, L. Pollegioni, P. D'Arrigo, E. Rosini, A novel, simple screening method for investigating the properties of lignin oxidative activity, Enzym. Microb. Technol. 96 (2017) 143–150.
[28] G.M.M. Rashid, T.D.H. Bugg, Enhanced biocatalytic degradation of lignin using combinations of lignin-degrading enzymes and accessory enzymes, Catal. Sci. Technol. 11 (2021) 3568–3577.
[29] C. Yang, R. Freudi, C. Qiao, A. Mulchandani, Cotranslocation of methyl parathion hydrolase to the periplasm and of organophosphorus hydrolase to the cell surface of *Escherichia coli* by the Tat Pathway and ice nucleation protein display system, Appl. Environ. Microbiol. 76 (2010) 434–440.
[30] R.S.Y. Wong, R.A. Wirtz, R.E.W. Hancock, *Pseudomonas aeruginosa* outer membrane protein OprF as an expression vector for foreign epitopes: the effects of positioning and length on the antigenicity of the epitope, Gene 158 (1995) 55–60.
[31] S.H. Lee, J.-I. Choi, M.-J. Han, J.H. Choi, S.Y. Lee, Display of lipase on the cell surface of *Escherichia coli* using OprF as an anchor and its application to enantioselective resolution in organic solvent, Biotech. Bioeng. 90 (2005) 223–230.
[32] D. Salvachúa, E.M. Karp, C.T. Nimlos, D.R. Vardon, G.T. Beckham, Towards lignin consolidated bioprocessing: simultaneous lignin depolymerization and product generation by bacteria, Green Chem. 17 (2015) 4951–4967.
[33] D.R. Vardon, M.A. Franden, C.W. Johnson, E.M. Karp, M.T. Guarnieri, J.G. Linger, M.J. Salm, T.J. Strathmann, G.T. Beckham, Adipic acid production from lignin, Energy Environ. Sci. 8 (2015) 617–628.
[34] M. Kohlstedt, S. Starck, N. Barton, J. Stolzenberger, M. Selzer, K. Mehlmann, S. Schneider, D. Pleissner, J. Rinkel, J.S. Dickschat, J. Venus, J.B.J.H. van Duuren, C. Wittmann, From lignin to nylon: cascaded chemical and biochemical conversion using metabolically engineered *Pseudomonas putida*, Metab. Eng. 47 (2018) 279–293.
[35] C.W. Johnson, D. Salvachúa, N.A. Rorrer, B.A. Black, D.R. Vardon, P.C. John St., N. S. Cleveland, G. Dominick, J.R. Elmore, N. Grundl, P. Khanna, C.R. Martinez, W. E. Michener, D.J. Peterson, K.J. Ramirez, P. Singh, T.A. VanderWall, A.N. Wilson, X. Yi, M.J. Biddy, Y.J. Bomble, A.M. Guss, G.T. Beckham, Innovative chemicals and materials from bacterial aromatic catabolic pathways, Joule 3 (2019) 1523–1537.
[36] H. Gómez-Álvarez, P. Iturbe, V. Rivero-Buceta, P. Mines, T.D.H. Bugg, J. Nogales, E. Díaz, Bioconversion of lignin-derived aromatics into the building block pyridine 2,4-dicarboxylic acid by engineering recombinant *Pseudomonas putida* strains, Bioresour. Technol. 346 (2022), 126638.
[37] S. Djebbar-Sid, O. Benali-Baitich, J.P. Deloume, Synthesis, characterization, electrochemical behaviour and catalytic activity of manganese(II) complexes with linear and tripodal tetradentate ligands derived from Schiff bases, Transit. Met. Chem. 23 (1998) 443–447.
[38] R. Varadarajan, T.E. Zewert, H.B. Gray, S.G. Boxer, Effects of buried ionizable amino acids on the reduction potential of recombinant myoglobin, Science 243 (1989) 69–72.
[39] P. Hosseinzadeh, E.N. Mirts, T.D. Pfister, Y.-G. Gao, C. Mayne, H. Robinson, E. Tajkhorshid, Y. Lu, Enhancing Mn(II)-binding and manganese peroxidase activity in a designed cytochrome c peroxidase through fine-tuning secondary-sphere interactions, Biochemistry 55 (2016) 1494–1502.